J. Biochem. **135**, 701–708 (2004)
DOI: 10.1093/jb/mvh085

Mutational and Structural-Based Analyses of the Osmolyte Effect on Protein Stability

Kazufumi Takano*[,1,2], Minoru Saito[3], Masaaki Morikawa[1] and Shigenori Kanaya[1]

[1]Department of Material and Life Science, Osaka University, 2-1 Yamadaoka, Suita, Osaka 565-0871; [2]Precursory Research for Embryonic Science and Technology (PRESTO), Japan Science and Technology Agency (JST), 2-1 Yamadaoka, Suita, Osaka 565-0871; and [3]Faculty of Science and Technology, Hirosaki University, 3 Bunkyo-cho, Hirosaki, Aomori 036-8561

Received March 26, 2004; accepted April 13, 2004

It is known that several naturally occurring substances known as osmolytes increase the conformational stability of proteins. Bolen and co-worker proposed the osmophobic theory, which asserts the osmolyte effect occurs because of an unfavorable interaction of osmolytes mainly with the protein backbone, based on the results on the transfer Gibbs energy of amino acids (Δg) [Bolen and Baskakov (2001) *J. Mol. Biol.* 310, 955–963]. In this paper, we report the effect of sarcosine on the conformational stability (ΔG) of RNase Sa (96 residues and one disulfide bond) and four mutant proteins. The thermal denaturation curves for RNase Sa in sarcosine fitted a two-state model on nonlinear least-squares analysis. All the RNase Sa proteins were stabilized by sarcosine. For example, the increase in stability of the wild-type protein in 4 M sarcosine due to the osmolyte effect ($\Delta_o\Delta G$) is 3.2 kcal/mol. Mutational analysis of the osmolyte effect indicated that the changed $\Delta_o\Delta G$ values upon mutation ($\Delta_m\Delta_o\Delta G$), as estimated from the Δg values, are similar to the experimental values. Structural-based analysis of the osmolyte effect was also performed using model denatured structures: (a) a fully extended model (single chain) with no disulfide bond, (b) two-part, unfolded models (two chains) with a disulfide bond constructed through molecular dynamic (MD) simulation, and (c) a two-part, folded model (two chains). The two-part, unfolded models were expected to be more suitable as denatured structures. The $\Delta_o\Delta G$ values calculated using the two-part, unfolded models were more consistent with experimental values than those calculated using the fully extended and two-part, folded models. This suggests that MD simulation is useful for testing denatured structures. These results indicate that the osmophobic theory can explain the osmolyte effect on protein stability.

Key words: accessible surface area, denatured state, mutant, Osmolyte, protein stability, RNase Sa, sarcosine.

Osmolytes, which are a class of small molecules used in nature by organisms to protect themselves from the stress of high osmotic pressure (*1*, *2*), have been found to stabilize the conformations of proteins. This stabilizing ability is known as the osmolyte effect (*3*, *4*). Osmolytes are divided into several types: sugars, methyl ammonium derivatives, amino acids and their derivatives, and polyhydric alcohols. The mechanism by which a protein is stabilized in the presence of an osmolyte, however, is not completely understood (*2*, *5*, *6*) and remains the subject of controversy (*4*, *7–10*).

Bolen and co-worker proposed the osmophobic theory (*11*), which asserts that the osmolyte effect on protein stability is due to a solvophobic thermodynamic force. The thermodynamic cycle of the osmolyte effect on protein stability is described in Scheme 1. ΔG^W and ΔG^O are the denaturation Gibbs energy changes in water (W) and the presence of an osmolyte (O), respectively. The osmolyte effects in both the denatured (D) and native (N) states ($\Delta_o G_D$ and $\Delta_o G_N$, respectively) can be estimated from the transfer Gibbs energies of proteins, from water to an osmolyte, based on solubility measurements. They measured the transfer Gibbs energies values of amino acids (Δg) in several osmolytes (*12*, *13*). In the presence of an osmolyte, the backbone of a protein is highly exposed

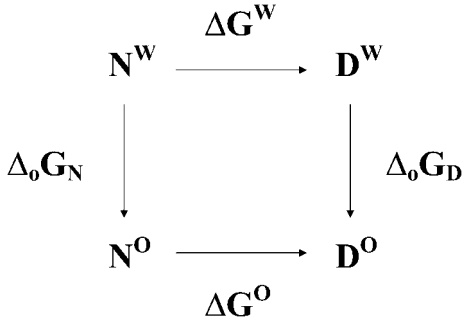

Scheme 1.

*To whom correspondence should be addressed at: Department of Material and Life Science, Osaka University; and PRESTO, JST. Tel: +81-6-6879-4157, Fax: +81-6-6879-4157, E-mail: ktakano@mls.eng.osaka-u.ac.jp

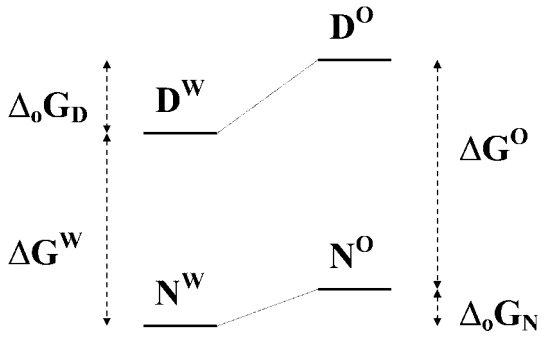

Fig. 1. **Relative Gibbs energy (ΔG) diagram for native (N) and denatured (D) states, from water (W) to osmolyte (O) solution.**

to the osmolyte in the denatured state; therefore, the destabilization of the denatured state due to unfavorable interaction between the osmolyte and the backbone is much greater than the destabilization of the native state. This results in enhancement of the protein stability, as shown in Fig. 1. Thus, the energy transfer data indicate that the osmophobic theory explains protein stabilization. There are, however, few reports in which the transfer Gibbs energy values estimated from the Δg values were used for the analysis of protein stability measurements in osmolytes. In such analysis, both denatured structure information and native structure information are needed. The transfer Gibbs energy values, from water to an osmolyte, of the denatured and native states were calculated using Eq. 1.

$$\Delta_0G_D \text{ or } \Delta_0G_N = \Sigma\ \alpha\ \Delta g \quad (1)$$

Here, α represents the fractional exposure of an amino acid residue in the native or denatured state against each amino acid, and Δg represents the transfer Gibbs energy of the amino acid. The α value for the native state (α_N) is obtained from the accessible surface areas (ASAs) of the amino acid residues in the native structure and the amino acids. In the case of the denatured state, we have to prepare a denatured structure for such analysis.

$$\alpha_N = \Sigma\ ASA_N/ASA_{amino} \quad (2)$$

$$\alpha_D = \Sigma\ ASA_D/ASA_{amino} \quad (3)$$

Here, ASA_{amino}, ASA_N, and ASA_D are the ASAs of an amino acid, the native state, and the denatured state, respectively.

Mutational analysis has often been used to elucidate the mechanism of stabilization of the conformations of proteins (*14–16*). One reason is that with this analysis one does not need to take the denatured state into account because of neutralization of the effect of the denatured structure. However, few studies involving mutant proteins to analyze the osmolyte effect have been reported. With mutational analysis of the osmolyte effect one is also able to cancel out the effect of the denatured state.

In this study, we measured the thermal denaturation of RNase Sa and four mutant proteins in the presence of sarcosine using circular dichroism (CD) in order to verify the osmophobic theory. RNase Sa has 96 residues and one disulfide bond. The stability of RNase Sa has been well examined. The Δg values of amino acids, from water to sarcosine, have been determined from solubility measurements (*12*). The four mutant proteins we used were V2T, L19K, I22K and A23K. Val 2, Leu 19 and Ile 22 are buried residues but Ala 23 is exposed to the solvent in the native structure. Figure 2 shows the structure of RNase Sa and the mutation sites. The stability of L19K and I22K is lower than that of the wild-type protein, but V2T and A23K exhibit similar stability to the wild-type. The difference in Δg value between Leu/Ile and Lys is bigger than that between Val and Thr, or between Ala and Lys. All the mutant proteins were stabilized by sarcosine. We analyzed the osmolyte effect on the stability of RNase Sa by means of transfer Gibbs energy using two different sets of information; the mutant data and model denatured structures. The model denatured structures were obtained by molecular dynamics (MD) simulation and used to roughly estimate the accessible surface area of the denatured state. We found that the osmophobic interaction clarifies the experimental observation of protein stability in the presence of osmolytes.

MATERIALS AND METHODS

Proteins—RNase Sa was expressed and purified as previously described (*17*, *18*). Protein concentrations were determined using a molar absorption coefficient at 278 nm of 12,300 M^{-1} cm^{-1}. The protein solutions were buffered at pH 7.0 with 30 mM MOPS buffer in the presence of various concentrations of sarcosine.

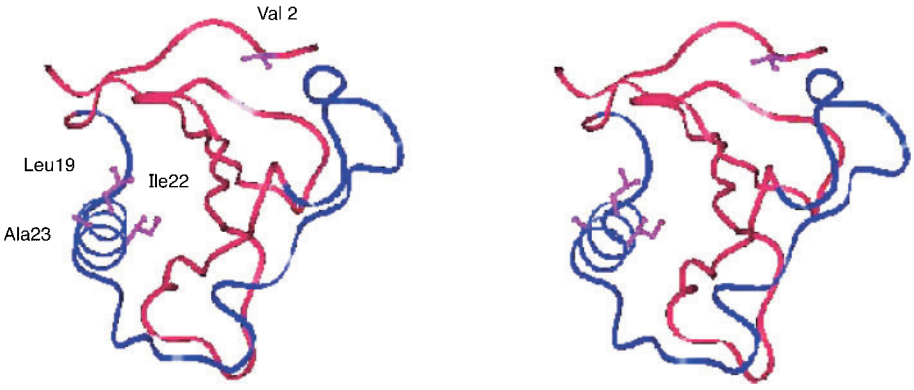

Fig. 2. **Stereo-structure of RNase Sa and the residues that have been substituted.** Part A (red) comprises residues 1–9 and 51–96, and Part B (blue) residues 10–50 (see text).

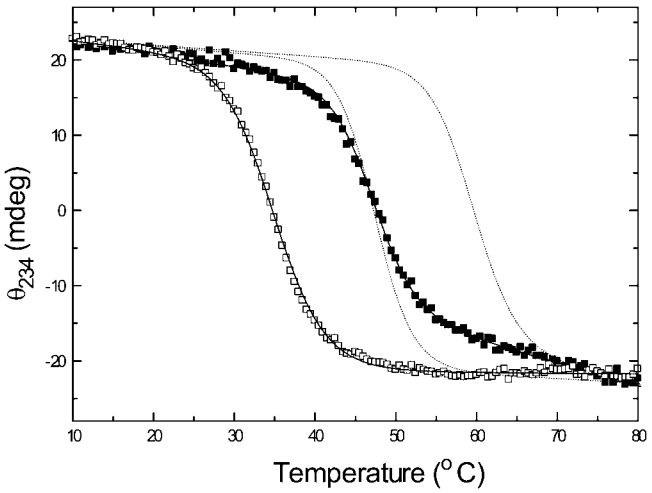

Fig. 3. **Typical thermal denaturation curves for I22K RNase Sa in the absence (open squares) and presence (filled squares) of 4 M sarcosine monitored by measuring the circular dichroism at 234 nm.** The continuous lines are theoretical curves based on Eq. 4. The dashed lines are the theoretical curves for wild-type RNase Sa.

Thermal Denaturation Determined by CD Measurement—CD measurements of the thermal denaturation of RNase Sa and the mutant proteins were performed on a Jasco J-725 spectropolarimeter (*19*). The thermal transition curves for RNase Sa proteins in the presence of various concentrations of sarcosine were monitored at 234 nm with a 2-mm path-length cell. The protein concentration was about 0.1 mg/ml. The heating rate was 1°C/min.

Nonlinear least-squares analysis was performed to fit the thermal denaturation data to Eq. 4 (*20*).

$$y = ((y_f + m_f\,[T]) + \exp((\Delta H_m/RT)\,((T - T_m)/T_m))\,(y_u + m_u\,[T]))/(1 + \exp((\Delta H_m/RT)\,((T - T_m)/T_m))) \quad (4)$$

Here, $y_f + m_f$ [T], and $y_u + m_u$ [T] describe the linear dependence of the pre- and post-transitional baselines on temperature, respectively, ΔH_m is the enthalpy of denaturation at T_m, and T_m is the midpoint of the thermal denaturation curve. Curve fitting was performed using MicroCal Origin curve-fitting software (MicroCal, Northampton, MA).

MD Simulation for the Model Denatured Structures of RNase Sa—RNase Sa was divided in to two parts, A and B. Part A (residues 1–9 and 51–96 with a disulfide bond) consists mainly of a β-sheet, and part B (residues 10–50) of an α-helix with a long arm. These parts were immersed in water spheres of 34-Å radius. Cut sections of the two parts (residues 9–10 and 50–51) were capped with an acetyl group (ACE) for the N-terminal side and with N-methylamide (NME) for the C-terminal side. The total numbers of solute atoms were 852 for part A and 613 for part B. The total numbers of water molecules were 5180 for part A and 5239 for part B. The force fields used were AMBER/all atom type (parm96) for the solute atoms (*21*, *22*) and SPC for the water molecules (*23*). To equilibrate whole systems in solution at 300 K, MD simulations were performed at 300 K initially for 10 ps with position constraints (harmonic potential of 10 kcal/mol/Å^2) for heavy atoms of the solutes and finally for 90 ps without any constraints. After the 300 K simulations, the temperatures of these systems were increased from 300 to 500 K to accelerate the unfolding process. Associated with the increase in temperature, the water spheres slightly expanded (from 34- to 36-Å radius) to compensate for the increase in pressure. The 500-K simulations were performed during 800 ps (from 100 to 900 ps). All MD simulations were performed with a VPP5000 with 8 processors and a COSMOS90 with the PPPC (Particle-Particle and Particle-Cell) method (*24*). Long-range Coulomb interactions were calculated using the PPPC method without truncation (*25*).

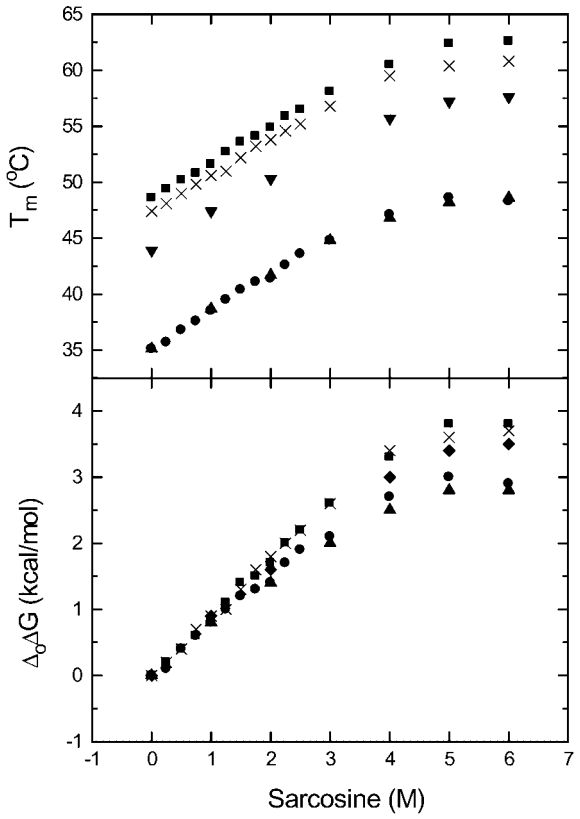

Fig. 4. **T_m (a) and $\Delta_o\Delta G$ (b) values as a function of the sarcosine concentration for wild-type and mutant RNase Sa; wild-type (crosses), V2T (inverted triangles), L19K (right triangles), I22K (circles), and A23K (squares).**

Calculation of ASA Values—The ASA values for each atom were calculated by the procedure previously described by Connolly (*26*) with probes of 1.4 Å (*27–29*). For calculation of the ASA values for the two-part unfolded and folded models of the denatured structures, the two parts (A: residues 1–9 and 51–96 with disulfide bond, B: residues 10–50) were separately calculated.

RESULTS

Thermal Denaturation of the Wild-Type RNase Sa in the Presence of Sarcosine—We examined the thermal denaturation of RNase Sa by means of CD in the presence of sarcosine. The CD measurements were carried out at pH 7.0, where the thermal denaturation of RNase

Table 1. **Thermodynamic parameters for thermal denaturation of wild-type RNase Sa in the presence of sarcosine.**

Sarcosine (M)	T_m [a] (°C)	$\Delta_o T_m$ [b] (°C)	ΔH_m [c] (kcal/mol)	ΔS_m [d] (cal/mol K)	$\Delta_o \Delta G$ [e] (kcal/mol)
0	47.4		89	278	
0.25	48.1	0.7	90	280	0.2
0.5	49.0	1.6	92	286	0.4
0.75	49.8	2.4	88	272	0.7
1.0	50.6	3.2	88	272	0.9
1.25	51.0	3.6	88	271	1.0
1.5	52.2	4.8	91	280	1.3
1.75	53.2	5.8	89	273	1.6
2.0	53.8	6.4	86	263	1.8
2.25	54.6	7.2	88	268	2.0
2.5	55.2	7.8	89	271	2.2
3.0	56.8	9.4	85	258	2.6
4.0	59.0	11.6	83	250	3.2
5.0	60.4	13.0	85	255	3.6
6.0	60.8	13.4	70	210	3.7

[a] $T_m = T$ where $\Delta G = 0$. The error is ± 0.3°C. [b] $\Delta_o T_m = T_{m\,(xM)} - T_{m\,(0M)}$. [c] ΔH_m = enthalpy of denaturation at T_m. The error is ± 4 kcal/mol. [d] $\Delta S_m = \Delta H_m / T_m$. ΔS_m is the entropy of denaturation at T_m. The error is ± 12 cal/mol K. [e] $\Delta_o \Delta G = \Delta_o T_m \Delta S_{m\,(0M)} = \Delta G_{(xM)} - \Delta G_{(0M)} = \Delta G^O - \Delta G^W$. The error is ± 0.1 kcal/mol. See Becktel and Schellman (*41*) or Pace and Scholtz (*42*) for a discussion of this method.

Table 2. **Thermodynamic parameters for yhermal denaturation of wild-type and mutant RNase Sa in the absence and presence (4 M) of sarcosine.**

	Sarcosine (M)	T_m (°C)	$\Delta_o T_m$ [a] (°C)	$\Delta_m T_m$ [b] (°C)	$\Delta_o \Delta G$ [c] (kcal/mol)	$\Delta_m \Delta G$ [d] (kcal/mol)
Wild-type	0	47.4				
	4.0	59.0	11.6		3.2	
V2T [e]	0	43.9		–3.5		–1.0
	4.0	55.7	11.8	–3.3	3.0	–0.8
L19K	0	35.1		–12.3		–3.4
	4.0	47.2	12.1	–11.8	2.6	–3.0
I22K	0	35.1		–12.3		–3.4
	4.0	47.1	12.0	–11.9	2.7	–3.0
A23K	0	48.6		1.2		0.3
	4.0	60.5	11.9	1.5	3.3	0.4

[a] $\Delta_o T_m = T_{m\,(4M)} - T_{m\,(0M)}$. [b] $\Delta_m T_m = T_{m\,(mutant)} - T_{m\,(wt)}$. [c] $\Delta_o \Delta G = \Delta_o T_m \Delta S_{m\,(0M)} = \Delta G_{(4M)} - \Delta G_{(0M)}$. The error is ± 0.1 kcal/mol. [d] $\Delta_m \Delta G = \Delta_m T_m \Delta S_{m\,(wt)} = \Delta G_{(mutant)} - \Delta G_{(wt)}$. The error is ± 0.1 kcal/mol. [e] Data in the absence of sarcosine are from Takano *et al.* (*43*).

Sa is very reversible. Figure 3 shows the thermal denaturation curves for RNase Sa in the absence and presence of 4 M sarcosine. In a previous study, RNase Sa was found to unfold reversibly through a two-state mechanism (*19*). We confirmed by checking reheated samples that, in the presence of sarcosine, the thermal denaturation of RNase Sa is reversible. The denaturation curves fitted to Eq. 4. It was assumed that the thermal transition curves for RNase Sa in sarcosine can be approximated by a two-state model. The thermodynamic parameters of wild-type RNase Sa with various concentrations of sarcosine at pH 7.0 are presented in Table 1, and the equations used to calculate these values are given in the footnotes to Table 1 (*16*). Here, we use the $\Delta_o \Delta G$ value to evaluate the relative stabilizing effect of sarcosine (*30*). Figures 4(a) and (b) show the T_m and $\Delta_o \Delta G$ values as a function of the sarcosine concentration. The T_m and $\Delta_o \Delta G$ values of wild-type RNase Sa increased to 13.4°C and 3.7 kcal/mol, respectively, as the concentration of sarcosine was increased from 0 to 6 M.

Thermal Denaturation of the Mutant RNase Sa in the Presence of Sarcosine—Figure 3 shows the thermal denaturation curves for I22K RNase Sa in the absence and presence of 4 M sarcosine. The thermal denaturation curves were obtained in the same way as for the wild-type protein. Figures 4(a) and (b) show the T_m and $\Delta_o \Delta G$ values as a function of the sarcosine concentration for the mutant proteins. The thermodynamic parameters of RNase Sa with 0 and 4 M sarcosine at pH 7.0 are summarized in Table 2. The effect of 4 M sarcosine on stability ($\Delta_o \Delta G$), which ranges from 2.6 to 3.3 kcal/mol, depends on the mutant proteins. The $\Delta_m \Delta G$ values show a difference in stability between the wild-type and mutant proteins.

Model Denatured Structures of RNase Sa—For convenience, when generating the model structures of the denatured state, RNase Sa was treated as the combination of the two components, *i.e.*, part A consisting of a β-sheet, and part B consisting of an α-helix with a long arm. These parts are tightly combined with each other through two hydrophobic clusters, like two snap fasteners. We produced models of the denatured-state structures between the native structure and the completely extended structure by means of MD simulations, as shown in Fig. 5. The model structure at the first stage

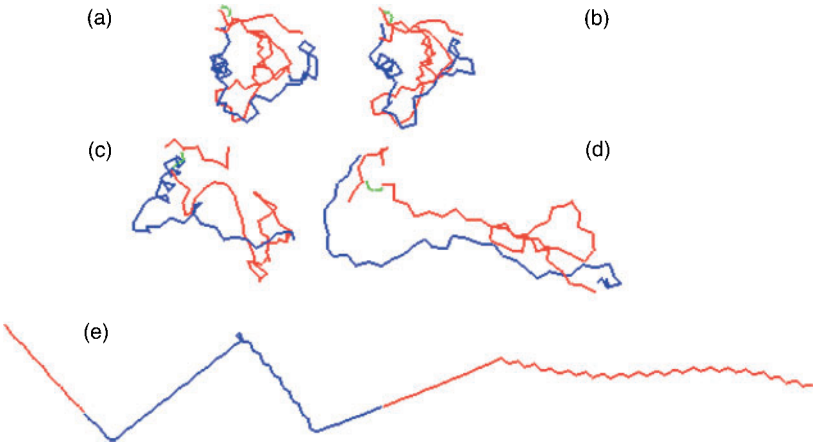

Fig. 5. **Model denatured structures of RNase Sa (Cα trace): (a) two-part, folded model; two-part, unfolded models with a disulfide bond constructed on MD simulation, (b) first stage, (c) second stage, (d) third stage; and (e) extended model with no disulfide bond.** Part A (red) comprises residues 1–9 and 51–96 with a disulfide bond (Cys 7–Cys 96) (green). Part B (blue) comprises residues 10–50. The disposition of parts A and B in (a) to (d) has no meaning.

comprises both parts A and B, equilibrated by MD means of simulations in solution at 300 K. This structure was supposed to mimic the situation in which the two hydrophobic clusters are broken due to water penetration, but the secondary structure is maintained. Model structures at the second and third stages are those obtained on 500 K simulations for 800 ps. We adopted the structures after the initial 400 ps simulation at 500 K as model structures of the second stage, and the last structures of the 500 K simulation as model structures of the third stage. The β-sheet in part A was almost broken at the second and third stages. The α-helix in part B remained at the second stage but had disappeared at the third stage. We adopted the completely extended structure without the disulfide bond as the model structure at the last stage.

DISCUSSION

Effect of Sarcosine on the Stability of RNase Sa—The present study showed that sarcosine stabilizes the conformations of RNase Sa and its mutant proteins. How are osmolytes such as sarcosine able to stabilize proteins? Based on an elegant series of experiments, Timasheff showed that osmolytes are preferentially excluded from the vicinity of a protein (*31*, *32*). Because the thermodynamic stability of proteins is determined by the delicate balance between the Gibbs energies of the native and denatured states, Bolen and co-worker proposed a thermodynamic cycle for the osmolyte effect on protein stability, as shown in Scheme 1 (*11*). This mechanism is identical to the approach by Nozaki and Tanford to understanding the effects of urea and guanidine hydrochloride on protein denaturation (*33*). With this approach, it is possible to predict the osmolyte stabilization of proteins from the transfer Gibbs energy, from water to an osmolyte, based on solubility measurements. The present findings regarding RNase Sa stability with osmolytes will lead to a better understanding of the role of osmolytes in protein stability. In the following sections, we will clarify the validity of the osmophobic theory by means of mutational- and structural-based analyses independently.

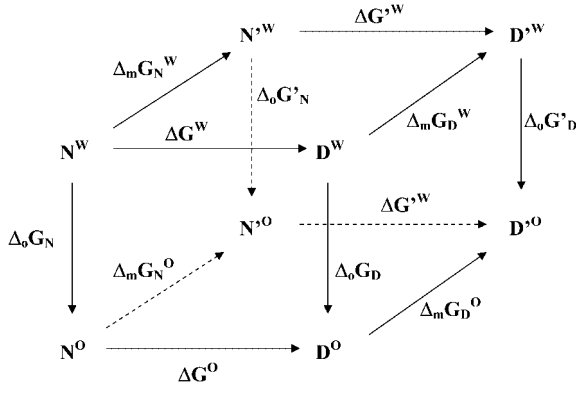

Scheme 2.

Mutational Analysis of the Osmolyte Effect on RNase Sa Stability in 4 M Sarcosine—Scheme 2 shows the thermodynamic cycle for mutational analysis of the osmolyte effect on the conformational stability of proteins. This scheme is based on Scheme 1, and is similar to the idea of a double-mutant cycle (*34*). The thermodynamic cycle of the osmolyte effect on protein stability in mutant proteins and the mutational effect are represented by the signs ' and Δ_m, respectively, in Scheme 2. According to the cycle, the changes in the $\Delta_o\Delta G$ value upon mutation ($\Delta_m\Delta_o\Delta G$) can be represented by the following equation, which is based on Eq. 1.

$$\begin{aligned}\Delta_m\Delta_o\Delta G &= \Delta_o\Delta G' - \Delta_o\Delta G \\ &= (\Delta_o G'_D - \Delta_o G'_N) - (\Delta_o G_D - \Delta_o G_N) \\ &= (\Sigma\, \alpha'_D\, \Delta g - \Sigma\, \alpha'_N\, \Delta g) - (\Sigma\, \alpha_D\, \Delta g - \Sigma\, \alpha_N\, \Delta g)\end{aligned} \quad (5)$$

Then, the effects of residues other than the mutated residue (X → Y) are cancelled out between the wild-type and mutant parameters.

$$\Delta_m\Delta_o\Delta G = \Delta g_Y\, (\alpha_D - \alpha_N)_Y - \Delta g_X\, (\alpha_D - \alpha_N)_X \quad (6)$$

Here, $(\alpha_N)_Y$ is nearly equal to $(\alpha_N)_X$, and we also assume that $(\alpha_D)_X$ and $(\alpha_D)_Y$ are almost 1 because the residue in the denatured state would be completely exposed.

$$\Delta_m\Delta_o\Delta G \approx (1 - \alpha_N)_X\, (\Delta g_Y - \Delta g_X) \quad (7)$$

Table 3 summarizes the $\Delta_m\Delta_o\Delta G$ values of the four mutant RNase Sa proteins in 4 M sarcosine determined in the experiments and by calculation with Eq. 7. There is good agreement in the $\Delta_m\Delta_o\Delta G$ values between the

Table 3. **$\Delta_m\Delta_o\Delta G$ values (kcal/mol) of RNase Sa mutants in 4 M sarcosine.**

	$\Delta_m\Delta_o\Delta G$	
	Experiment[a]	Calculation[b]
V2T	–0.2	–0.2
L19K	–0.6	–0.3
I22K	–0.5	–0.4
A23K	0.1	0

[a]Eq. 5. ($\Delta_m\Delta_o\Delta G = \Delta_o\Delta G' - \Delta_o\Delta G = \Delta_o\Delta G_{(mutant)} - \Delta_o\Delta G_{(WT)}$). The error is ± 0.1 kcal/mol. [b]Eq. 7. [$\Delta_m\Delta_o\Delta G \approx (1 - \alpha_N)_X (\Delta g_Y - \Delta g_X)$].

Table 4. **$\Delta_o\Delta G$ nvalues (kcal/mol) of RNase Sa mutants in 4 M sarcosine.**

	Stage	$\Delta_o\Delta G$		
		Part A	Part B	Whole
Experiment[a]				3.2
Calculation[b]				
Two-Part folded model		0.8	1.0	1.8
Two-Part unfolded model	First	1.0	1.5	2.5
	Second	1.7	1.5	3.2
	Third	2.2	3.2	5.4
Extend model (no disulfide bond)				5.9

[a]$\Delta_o\Delta G = \Delta G_{(4M)} - \Delta G_{(0M)}$. The error is ± 0.1 kcal/mol. [b]$\Delta_o\Delta G = \Sigma\, \Delta g\, [(ASA_D - ASA_N)/ASA_{amino})]$. For the two-part unfolded and folded models, the ASA values of the two parts (A, residues 1–9 and 51–96 with disulfide bond; B, residues 10–50) were separately calculated.

experiments and calculation. The results indicate that the observation of osmolyte stabilization of proteins is in qualitative accord with the prediction based on the osmophobic theory.

For L19K, the $\Delta_m\Delta_o\Delta G$ value was slightly different between the experiments and calculation, compared with the other mutants. This might be because of the structural change in the native state upon mutation. Because the side chain of Leu 19 points toward the core in the native structure (*35*), the longer side chain of Lys 19 in the mutant structure would cause some structural changes. On the other hand, Val 2 and Ile 22 are buried residues, but their side chains are located near the surface of the protein, resulting in subtle structural changes upon mutation.

Structure-Based Analysis of the Osmolyte Effect on RNase Sa Stability in 4 M Sarcosine—The $\Delta_o\Delta G$ value, which reflects the relative stabilizing effect of an osmolyte, is obtained using Scheme 1 and Eqs. 1–3 as follows.

$$\begin{aligned}\Delta_o\Delta G &= \Delta G^O - \Delta G^W \\ &= \Delta_o G_D - \Delta_o G_N \\ &= \Sigma\, \alpha_D\, \Delta g - \Sigma\, \alpha_N\, \Delta g \\ &= \Sigma\, \Delta g\, (\alpha_D - \alpha_N) \\ &= \Sigma\, \Delta g\, ((ASA_D - ASA_N)/ASA_{amino}) \end{aligned} \quad (8)$$

With this analysis, the $\Delta_o\Delta G$ value calculated with Eq. 8 is highly dependent on the denatured structure. The largest number of the residues would be exposed to the solvent in the denatured state, although not all residues would be exposed, because RNase Sa has one disulfide bond which restricts the conformation of the denatured state. The effect of each residue might be small, but the accumulated effect of all residues will be large. In this work, we constructed several types of denatured models to roughly estimate the accessible surface area of the denatured state: (a) a fully extended model with no disulfide bond, (b) two-part, unfolded models with the disulfide bond at varying stages of MD simulation, and (c) a two-part, folded model. The two-part, unfolded models were expected to be more suitable denatured structures. The $\Delta_o\Delta G$ values calculated with Eq. 8 using several model denatured structures are summarized in Table 4.

The order of the ASAs is the extended model; the two-part, unfolded model at the third, second and first stages; and the two-part, folded model. The order of the calculated $\Delta_o\Delta G$ values is the same as that of the ASAs, depending on the calculated $\Delta_o\Delta G$ value for the ASA value of the denatured structure. The actual denatured structure is expected to lie between the two-part folded and extended models, such as the two-part, unfolded model. The experimental $\Delta_o\Delta G$ value, 3.2 kcal/mol, lies between the calculated $\Delta_o\Delta G$ values for the two-part folded and extended models, 1.8 and 5.9 kcal/mol, respectively. This suggests that the osmophobic theory suitably explains the osmolyte effect on protein stability.

The experimental $\Delta_o\Delta G$ value, 3.2 kcal/mol, is more similar to the calculated $\Delta_o\Delta G$ value, 3.2 kJ/mol, with the two-part, unfolded model at the second stage. This means that there is consistency between the experiments and MD simulations. The model structures at the other stages gave very different $\Delta_o\Delta G$ values: 2.5 for the first stage, 5.4 for the third stage, and 5.9 kcal/mol for the last stage. The second stage has a larger $\Delta_o\Delta G$ than the first stage, because of destruction of the β-sheet, and has a smaller $\Delta_o\Delta G$ than the third stage, because the α-helix remained. Therefore, our results suggest that the α-helix might be maintained in the denatured state (*36*, *37*). However, our present study does not rule out the possibility that a non-native hydrophobic cluster is formed in the denatured state. It is also possible to obtain other denatured structures with similar ASA values. Our model structures have been used to obtain a rough structure for the denatured state.

A denatured structure is important for analyzing protein stability and folding (*38–40*). However, it is quite difficult to determine denatured structures. Furthermore, we are not able to predict or even imagine a rough structure of a denatured state. If the osmophobic theory is correct, structural-based analysis of the osmolyte effect on protein stability, as shown in this paper, will provide an image of a denatured structure, such as the two-part, unfolded model of RNase Sa.

CONCLUSION

In this paper, we examined the osmophobic theory using the thermodynamic data on RNase Sa and its mutants in the presence of sarcosine, and we also examined model denatured structures. The results show that the osmolyte effect on protein stability can be explained by the osmophobic theory. Furthermore, information on a denatured structure became available on the structural-based analysis of the osmolyte effect on protein stability.

This work was supported in part by a Grant-in-Aid for Scientific Research on Priority Areas (C), 'Genome Information Science', from the Ministry of Education, Culture, Sports, Science and Technology of Japan (K.T. and M.S.), and by a Grant-in-Aid for National Project on Protein Structural and Functional Analyses from the Ministry of Education, Culture, Sports, Science and Technology of Japan (S.K.).

We wish to thank Dr. Nick Pace for critical reading of the manuscript and the helpful discussions.

REFERENCES

1. Yancey, P.H. and Somero, G.N. (1979) Counteraction of urea destabilization of protein structure by methylamine osmoregulatory compounds of elasmobranch fishes. *Biochem. J.* **183**, 317–323
2. Yancey, P.H., Clark, M.E., Hand, S.C., Bowlus, R.D., and Somero, G.N. (1982) Living with water stress: evolution of osmolyte systems. *Science* **217**, 1214–1222
3. Santoro, M.M., Liu, Y., Khan, S.M., Hou L.X., and Bolen D.W. (1992) Increased thermal stability of proteins in the presence of naturally occurring osmolytes. *Biochemistry* **31**, 5278–5283
4. Timasheff, S.N. (1993) The control of protein stability and association by weak interactions with water: how do solvents affect these processes? *Annu. Rev. Biophys Biomol. Struct.* **22**, 67–97
5. Arakawa, T. and Timasheff, S.N. (1985) The stabilization of proteins by osmolytes. *Biophys. J.* **47**, 411–414
6. Plaza del Pino, I.M. and Sanchez-Ruiz, J.M. (1995) An osmolyte effect on the heat capacity change for protein folding. *Biochemistry* **34**, 8621–8630
7. Shearwin, K.E. and Winzor, D.J. (1988) Effect of sucrose on the dimerization of alpha-chymotrypsin. Allowance for thermodynamic nonideality arising from the presence of a small inert solute. *Biophys. Chem.* **31**, 287–294
8. Berg, O.G. (1990) The influence of macromolecular crowding on thermodynamic activity: solubility and dimerization constants for spherical and dumbbell-shaped molecules in a hard-sphere mixture. *Biopolymers* **30**, 1027–1037
9. Parsegian, V.A., Rand, R.P., and Rau, D.C. (2000) Osmotic stress, crowding, preferential hydration, and binding: A comparison of perspectives. *Proc. Natl Acad. Sci. USA* **97**, 3987–3992
10. Davis-Searles, P.R., Saunders, A.J., Erie, D.A., Winzor, D.J., and Pielak, G.J. (2001) Interpreting the effects of small uncharged solutes on protein-folding equilibria. *Annu. Rev. Biophys Biomol. Struct.* **30**, 271–306
11. Bolen, D.W. and Baskakov, I.V. (2001) The osmophobic effect: natural selection of a thermodynamic force in protein folding. *J. Mol. Biol.* **310**, 955–963
12. Liu, Y. and Bolen, D.W. (1995) The peptide backbone plays a dominant role in protein stabilization by naturally occurring osmolytes. *Biochemistry* **34**, 12884–12891
13. Qu, Y., Bolen C.L., and Bolen, D.W. (1998) Osmolyte-driven contraction of a random coil protein. *Proc. Natl Acad. Sci. USA* **95**, 9268–9273
14. Yutani, K., Ogasahara, K., Tsujita, T., and Sugino Y. (1987) Dependence of conformational stability on hydrophobicity of the amino acid residue in a series of variant proteins substituted at a unique position of tryptophan synthase alpha subunit. *Proc. Natl Acad. Sci. USA* **84**, 4441–4444
15. Takano, K., Ogasahara, K., Kaneda, H., Yamagata, Y., Fujii, S., Kanaya, E., Kikuchi M., Oobatake, M., and Yutani, K. (1995) Contribution of hydrophobic residues to the stability of human lysozyme: calorimetric studies and X-ray structural analysis of the five isoleucine to valine mutants. *J. Mol. Biol.* **254**, 62–76
16. Pace, C.N., Horn, G., Hebert, E.J., Bechert, J., Shaw, K., Urbanikova, L., Scholtz, J.M., and Sevcik, J. (2001) Tyrosine hydrogen bonds make a large contribution to protein stability. *J. Mol. Biol.* **312**, 393–404
17. Hebert, E.J., Grimsley, G.R., Hartley, R.W., Horn, G., Schell, D., Garcia, S., Both, V., Sevcik, J., and Pace, C.N. (1997) Purification of ribonucleases Sa, Sa2, and Sa3 after expression in *Escherichia coli*. *Protein Expr. Purif.* **11**, 162–168
18. Hebert, E.J., Giletto, A., Sevcik, J., Urbanikova, L., Wilson, K.S., Dauter, Z., and Pace, C.N. (1998) Contribution of a conserved asparagine to the conformational stability of ribonucleases Sa, Ba, and T1. *Biochemistry* **37**, 16192–16200
19. Pace, C.N., Hebert, E.J., Shaw, K.L., Schell, D., Both, V., Krajcikova, D., Sevcik, J., Wilson, K.S., Dauter, Z., Hartley, R.W., and Grimsley, G.R. (1998) Conformational stability and thermodynamics of folding of ribonucleases Sa, Sa2 and Sa3. *J. Mol. Biol.* **279**, 271–286
20. Santoro, M.M. and Bolen, D.W. (1988) Unfolding free energy changes determined by the linear extrapolation method. 1. Unfolding of phenylmethanesulfonyl alpha-chymotrypsin using different denaturants. *Biochemistry* **27**, 8063–8068
21. Cornell, W.D., Cieplak, P., Bayly, C.I., Gould, I.R., Merz, K.M. Jr., Ferguson, D.M., Spellmeyer, D.C., Fox, T., Caldwell, J.W., and Kollman, P.A. (1995) A second generation force field for the simulation of proteins, nucleic acids, and organic molecules. *J. Amer. Chem. Soc.* **117**, 5179–5197
22. Kollman, P.A, Dixon, R., Cornell, W., Fox, T., Chipot, C., and Pohorille, A. (1997) Computer simulations of biomolecular systems (Wilkinson, A., Weiner, P., and van Gunsteren, W.F., ed.), vol. **3**, pp. 83–96, Elsevier
23. Berendsen, H.J.C., Postma, J.P.M, van Gunsteren, W.F., and Hermans, J. (1981) Interaction models for water in relation to protein hydration in *Intermolecular Forces Reidel* (Pullman, B., ed.) pp. 331–342, Dordrecht
24. Saito, M. (1992) Molecular dynamic simulations of proteins in water without the truncation of long-range Coulomb interactions. *Mol. Simul.* **8**, 321–333
25. Saito, M. (1994) Molecular dynamic simulations of proteins in solution: artifacts caused by the cutoff approximation. *J. Chem. Phys.* **101**, 4055–4061
26. Connolly, M.L. (1993) The molecular surface package. *J. Mol. Graph.* **11**, 139–141
27. Takano, K., Funahashi, J., Yamagata, Y., Fujii, S., and Yutani, K. (1997) Contribution of water molecules in the interior of a protein to the conformational stability. *J. Mol. Biol.* **274**, 132–142
28. Takano, K., Yamagata, Y., and Yutani, K. (1998) A general rule for the relationship between hydrophobic effect and conformational stability of a protein: stability and structure of a series of hydrophobic mutants of human lysozyme. *J. Mol. Biol.* **280**, 749–761
29. Funahashi, J., Takano, K., Yamagata, Y., and Yutani, K. (1999) Contribution of amino acid substitutions at two different interior positions to the conformational stability of human lysozyme. *Protein Eng.* **12**, 841–850
30. Gekko, K. and Timasheff, S.N. (1981) Thermodynamic and kinetic examination of protein stabilization by glycerol. *Biochemistry* **20**, 4677–4686
31. Timasheff, S.N. (2002) Protein hydration, thermodynamic binding, and preferential hydration. *Biochemistry* **41**, 13473–13482
32. Timasheff, S.N. (2002) Protein-solvent preferential interactions, protein hydration, and the modulation of biochemical reactions by solvent components. *Proc. Natl Acad. Sci. USA* **99**, 9721–9726
33. Nozaki, Y. and Tanford, C. (1963) The solubility of amino acids and related compounds in aqueous urea solutions. *J. Biol. Chem.* **238**, 4074–4080
34. Fersht, A.R., Matouschek A., and Serrano, L. (1992) The folding of an enzyme. I. Theory of protein engineering analysis of stability and pathway of protein folding. *J. Mol. Biol.* **224**, 771–782
35. Sevcik, J., Dauter, Z., Lamzin, V.S., and Wilson, K.S. (1996) Ribonuclease from *Streptomyces aureofaciens* at Atomic Resolution. *Acta Crystallogr.* **D52**, 327–344

36. Ueda, T., Nagata, M., and Imoto, T. (2001) Aggregation and chemical reaction in hen lysozyme caused by heating at pH 6 are depressed by osmolytes, sucrose and trehalose. *J. Biochem.* **130**, 491–496
37. Klein-Seetharaman, J., Oikawa, M., Grimshaw, S.B., Wirmer, J., Duchardt, E., Ueda, T., Imoto, T., Smith, L.J., Dobson, C.M., and Schwalbe, H. (2002) Long-range interactions within a non-native protein. *Science* **295**, 1719–1722
38. Mayor, U., Guydosh, N.R., Johnson, C.M., Grossmann, J.G., Sato, S., Jas, G.S., Freund, S.M., Alonso, D.O., Daggett, V., and Fersht, A.R. (2003) The complete folding pathway of a protein from nanoseconds to microseconds. *Nature*, **421**, 863–867
39. Shortle, D. (2002) Propensities, probabilities, and the Boltzmann hypothesis. *Adv. Protein Chem.* **62**, 1–23
40. Ohnishi, S. and Shortle, D. (2003) Effects of denaturants and substitutions of hydrophobic residues on backbone dynamics of denatured staphylococcal nuclease. *Protein Sci.* **12**, 1530–1537
41. Becktel, W.J. and Schellman, J.A. (1987) Protein stability curves. *Biopolymers* **26**, 1859–1877
42. Pace, C.N. and Scholtz, J.M. (1997) Measuring the conformational stability of a protein in *Protein Structure: A Practical Approach* (Creighton, T.E., ed.) pp. 299–321, Oxford IRL Press
43. Takano, K., Scholtz, J.M., Sacchettini, J., and Pace, C.N. (2003) The contribution of polar group burial to protein stability is strongly context-dependent. *J. Biol. Chem.* **278**, 31790–31795